A FEM Based Shell Solver—Final Report

Yuchen Su
2022013267
suyc22@mails.tsinghua.edu.cn

MingXuan Liu
2022012067
liu-mx22@mails.tsinghua.edu.cn

I. Introduction

Thin shells are slender, flexible structures characterized by a high width-to-thickness ratio (greater than 100). They are ubiquitous in both natural and engineered systems, from the delicate curvature of leaves to the structural components of vehicles and architecture. Unlike flat plates or fully volumetric solids, the mechanical behavior of thin shells is dominated by their intrinsic curvature, making accurate simulation particularly challenging and computationally demanding.

In this project, we develop a finite element method (FEM)-based solver implemented with taichi for simulating the elastic deformation of thin shells, centered around the Discrete Shells framework introduced by [1].

II. Related Works

A. Large timesteps in cloth simulation

The work [2] introduced a foundational approach for simulating cloth that remains influential in the field. By formulating the cloth dynamics as a system of differential equations and solving them implicitly, they achieved stability even under large timesteps.

B. Discrete Shells

The Discrete Shells model by [Grinspun et al. 2003]. provides a geometrically intuitive and computationally efficient framework for simulating thin shells. It discretizes the shell surface as a triangle mesh and models the mechanical behavior using discrete analogues of bending and membrane energies. Discrete Shells excels at preserving isometry during deformation and is particularly well-suited for thin, highly flexible materials where thickness is negligible.

III. Method

A. The Energy Model of Discrete Shells

a) Membrane Energy:

$$W_L = \sum_e (1 - ||e||/||\bar{e}||)^2 ||\bar{e}||$$

$$W_A = \sum_A (1 - ||A||/||\bar{A}||)^2 ||\bar{A}||$$

b) Bending Energy:

$$W_B(x) = \sum_e (\theta_e - \bar{\theta}_e)^2 ||\bar{e}||/\bar{h}_e$$

where θ_e and $\bar{\theta}_e$ are the corresponding complements of the dihedral angle of edge e measured in the deformed and undeformed configuration respectively, and $\bar{h}_e$ is a third of the average of the heights of the two triangle incidents to the edge.

c) dynamic system: Then, the system needed to be solved will be

$$(\mathbf{I} - \Delta t \mathbf{W}\frac{\partial \mathbf{f}}{\partial \mathbf{v}} - (\Delta t)^2 \mathbf{W}\frac{\partial \mathbf{f}}{\partial \mathbf{x}})\Delta \mathbf{v} = \Delta t \mathbf{W}(\mathbf{f}_0 + \Delta t \frac{\partial \mathbf{f}}{\partial \mathbf{x}}\mathbf{v}_0) + \mathbf{z}$$

We use the modified Conjugate Gradient Method to solve the system.

d) Collision: For most of the model, we use a collision model porposed by

$$v_{filterd} = v - nn^T v$$

with n the contact norm

e) pipeline: We use taichi for the whole implementation. We do not use the autodiff of taichi as taichi does not provide auto hessian, and we need preliminary information on the gradient for the hessian.

The whole pipeline is in Algorithm 1.

Algorithm 1 Shell Solver

$\mathbf{x} \leftarrow x^t$
Detect collisions and generate penalty constraints.
Compute $C(\mathbf{x})$, internal forces $\mathbf{f}_i$ and damping $\mathbf{d}_i$
Assemble global system (forces $\mathbf{f}$, stiffness $\mathbf{K}_{ij}$)
Add boundary and collision constraints
Solve linear system using modified-PCG
Update positions: $\mathbf{x}^{t+1} \leftarrow \mathbf{x}^t + \Delta \mathbf{x}$
Update velocities: $\mathbf{v}^{t+1} \leftarrow (\mathbf{x}^{t+1} - \mathbf{x}^t)/\Delta t$
return $\mathbf{x}^{t+1}$

IV. Results

A. Demonstation of the cloth solver

We simulate a piece of cloth undergoing free fall onto a sphere, with one edge constrained. The results are shown in Figure 2a and 2b

After testing the cloth solver, we replaced the membrane and bending models with those proposed in the Discrete Shells formulation. The updated simulation results are presented below.

B. Beam with Different Stiffness

We replicate the experiment described in the original article to evaluate the deformation behavior of a beam under varying stiffness values. Our results, shown as Fig 2, are qualitatively consistent with those reported in the article.

(a) Free falling cloth onto a ball

(b) Constrained cloth falling onto a ball

Fig. 1: Demonstration of the cloth solver

(a) $k_B = 10.0$ (b) $k_B = 1.0$ (c) $k_B = 0.1$

Fig. 2: beam with different stiffness

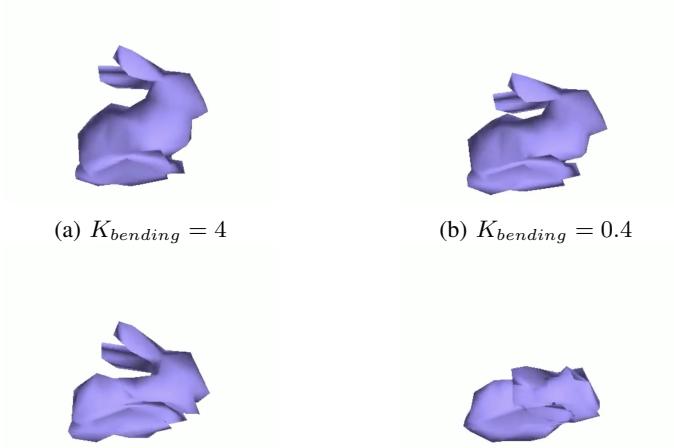

(a) $K_{bending} = 4$ (b) $K_{bending} = 0.4$

(c) $K_{bending} = 0.04$ (d) $K_{bending} = 0.004$

Fig. 3: Falling bunnies with different bending stiffnesss

C. Falling Bunny

Next, we simulate a more complex scenario: the free fall and subsequent bouncing of the Stanford Bunny. The simulation results under different stiffness values are shown in Figure 3.

However, as we increased the number of vertices in the Stanford Bunny, the simulation became unstable and eventually exploded during the free fall phase. Upon investigation, we identified the cause to be numerical instability in the `arccos` function. To address this issue, we switched from single-precision (fp32) to double-precision (fp64) floating-point arithmetic, which successfully resolved the problem.

D. Bouncing Bunny

Then, we attempt to adopt the Incremental Potential Contact (IPC) [3]framework to simulate the bouncing behavior between two Stanford Bunnies — a more challenging and contact-dense scenario. IPC is particularly appealing for our case because it enables robust, intersection-free collision handling through a carefully designed barrier energy formulation.

To achieve this, we use the following collision energy model:

$$b(d, \hat{d}) = \begin{cases} -(d - \hat{d})^2 \ln\left(\frac{d}{\hat{d}}\right), & 0 < d < \hat{d} \\ 0, & d \geq \hat{d} \end{cases}$$

where d is the current distance between two potentially colliding primitives (e.g., vertex-face or edge-edge), and $\hat{d}$ is the activation distance threshold.

We perform a line search over both the time step Δt and the contact stiffness parameter κ, in order to find values that minimize the total potential energy while ensuring that no intersections occur during the simulation.

E. Comparison with Abaqus

To test the accuracy of our FEM solver, we constructed a model of a lidless can, subjected it to compression in our simulator, and compared the results with those obtained from a more advanced FEM tool—Abaqus, which is shown in 4

For convenience, we applied a force constraint in the Abaqus simulations instead of a velocity constraint. Although our simulation contains some unrealistic aspects, we observed the same cyclic indentation along the edge, which validates the key deformation behavior and supports the credibility of our solver. [1]

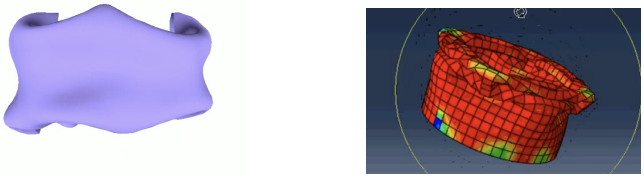

(a) ours (b) Abaqus

Fig. 4: Comparison between ours & Abaqus

V. Conclusions

We developed a shell solver using Taichi based on the Discrete Shells formulation. To validate the correctness of our implementation, we conducted a series of experiments and compared the performance of different numerical methods. Our results demonstrate that using double-precision floating-point arithmetic becomes crucial as the number of vertices increases, due to accumulated numerical errors.

Future improvements include supporting a wider variety of materials and incorporating techniques from recent research to enhance both the accuracy and performance of the solver and also incorporation of IPC.

[1]The reulte of abaqus simulation is borrowed from https://www.youtube.com/watch?v=29XRT5USQxo&themeRefresh=1

REFERENCES

[1] E. Grinspun, A. N. Hirani, M. Desbrun, and P. Schröder, "Discrete shells," in *Proceedings of the 2003 ACM SIGGRAPH/Eurographics Symposium on Computer Animation*, ser. SCA '03. Goslar, DEU: Eurographics Association, 2003, p. 62–67.

[2] D. Baraff and A. Witkin, "Large steps in cloth simulation," in *Proceedings of the 25th Annual Conference on Computer Graphics and Interactive Techniques*, ser. SIGGRAPH '98. New York, NY, USA: Association for Computing Machinery, 1998, p. 43–54. [Online]. Available: https://doi.org/10.1145/280814.280821

[3] M. Li, Z. Ferguson, T. Schneider, T. Langlois, D. Zorin, D. Panozzo, C. Jiang, and D. M. Kaufman, "Incremental potential contact: intersection-and inversion-free, large-deformation dynamics," *ACM Trans. Graph.*, vol. 39, no. 4, Aug. 2020. [Online]. Available: https://doi.org/10.1145/3386569.3392425

[4] R. Tamstorf and E. Grinspun, "Discrete bending forces and their jacobians," *Graph. Models*, vol. 75, no. 6, p. 362–370, Nov. 2013. [Online]. Available: https://doi.org/10.1016/j.gmod.2013.07.001

[5] E. Grinspun, "A discrete model of thin shells," in *ACM SIGGRAPH 2005 Courses*, ser. SIGGRAPH '05. New York, NY, USA: Association for Computing Machinery, 2005, p. 4–es. [Online]. Available: https://doi.org/10.1145/1198555.1198663

[6] T. Kim and D. Eberle, "Dynamic deformables: implementation and production practicalities," in *ACM SIGGRAPH 2020 Courses*, ser. SIGGRAPH '20. New York, NY, USA: Association for Computing Machinery, 2020. [Online]. Available: https://doi.org/10.1145/3388769.3407490